

# UCLA

## UCLA Previously Published Works

### Title

Quantification of Malondialdehyde in Atmospheric Aerosols: Application of the Thiobarbituric Acid Method

### Permalink

<https://escholarship.org/uc/item/7832q019>

### Journal

Aerosol and Air Quality Research, 22(7)

### ISSN

1680-8584

### Authors

Gonzalez, David H  
Paulson, Suzanne E

### Publication Date

2022

### DOI

10.4209/aaqr.220037

Peer reviewed

1           **Quantification of Malondialdehyde in Atmospheric Aerosols:**  
2                   *Application of the Thiobarbituric Acid Method*

3  
4                   **David H. Gonzalez, and Suzanne E. Paulson\***

5  
6           <sup>1</sup>*University of California at Los Angeles, Department of Atmospheric and Oceanic Sciences,*  
7                   *405 Hilgard Ave., Los Angeles, CA 90405*

8  
9                   \*Corresponding Author. Tel: 310-206-4442; Fax: 310-206-5219

10                   E-mail address: paulson@atmos.ucla.edu

11   **Abstract**

12  
13   Based on available toxicity data, malondialdehyde (MDA;  $O=CHCH_2CH=O$ ) has been  
14   designated as a potential human carcinogen. A handful of studies suggest that MDA forms in  
15   the gas and aerosol phase in the troposphere, potentially contributing to inhalation toxicity, yet  
16   it has never been quantified in ambient air. The thiobarbituric acid (TBA) acid assay for (MDA)  
17   has been used as a marker for reactive oxygen species (ROS), oxidative stress, and lipid  
18   peroxidation in biological samples for decades. Here we apply the TBA assay to estimate the  
19   amount of MDA in ambient fine particulate matter (PM<sub>2.5</sub>) for the first time, in samples  
20   containing biomass burning/urban aerosol from Fresno, CA, and urban aerosol from Los  
21   Angeles. We found 0.31– 0.75 ng m<sup>-3</sup> MDA in the particle phase, similar to the low end, but  
22   about to three orders of magnitude lower than the upper end of reported concentrations of the  
23   common C<sub>3</sub> oxygenates methylglyoxal and malonic acid. Additionally, we investigated the  
24   response in the assay to seven common small oxygenates, and found interference only from  
25   acrolein, and that only when the acrolein was at millimolar concentrations, well above expected  
26   levels in aerosol extracts. In sum, this work suggests that MDA is present at moderate levels in  
27   biomass burning and urban aerosols; more may be in the gas phase.

28  
29   **Keywords:** Carbonyl Quantification, Biomass Burning, Urban Aerosol, Aerosol Toxicity,  
30   Assay Interference.

31  
32  
33  
34  
35  
36  
37  
38  
39  
40

## 41 1. INTRODUCTION

42 Malondialdehyde (MDA) has been widely used as an indicator of aqueous reactive  
43 oxygen species (ROS), lipid peroxidation, oxidative stress, and rancidity in food products  
44 (Buege and Aust 1978, Halliwell and Gutteridge 1981, Zeb and Ullah 2016, Agarwal and  
45 Majzoub 2017). MDA is a product of lipid peroxidation (Buege and Aust 1978, Del Rio et al.  
46 2005). and OH-mediated oxidation of 2-deoxyribose, and it has been widely used to assess  
47 oxidation in human, animal, and ecotoxicity applications (Halliwell and Gutteridge 1981,  
48 Gutteridge and Halliwell 1988, Genaro-Mattos et al. 2009). MDA has also been shown to be  
49 mutagenic and carcinogenic, resulting in its classification as a possible human carcinogen  
50 (Millar 1991), and to contribute to atherosclerosis, suggesting a role more significant than  
51 simply an indicator for oxidation in biological systems (Basu and Marnett 1983, Niedernhofer  
52 et al. 2003, Del Rio et al. 2005, Papac-Milicevic et al. 2016).

53 Two studies have reported formation of gas phase MDA formation in laboratory  
54 organic photooxidation experiments. Liu et al. (1999) observed MDA formation from  
55 photooxidation of several aromatic oxidation products including 2-butenedial, 4-oxo-pentenal,  
56 and 1,3-butadiene in the gas phase in an environmental chamber. Zhou et al. (2014) found that  
57 ozonolysis of polyunsaturated fatty acids at the surface of an aqueous layer produces gaseous  
58 MDA. Furthermore, Beeby et al. (1987) found that photolysis of glycolaldehyde in aqueous  
59 solutions produced MDA, suggesting MDA can also form in bulk aerosol or cloud water.

60 Destailats et al. (2002) reported identification of MDA in ambient air in San Francisco,  
61 CA, using a derivatization method coupled with High-Resolution Gas Chromatography/Ion  
62 Trap Mass Spectrometry. The authors stated that MDA co-eluted with an internal standard that  
63 was distinguishable by interpreting a combination of electron ionization, methane chemical

64 ionization and derivative chemical ionization spectra. Their experimental design was not able  
65 to quantify its concentration and did not distinguish between gas or particle phase MDA.

66 Okochi and Brimblecombe (2002) used a bond contribution method to estimate a  
67 Henry's Law Constant for gas-particle partitioning for MDA, estimating a value of  $1.4 \times 10^4 \text{ M}$   
68  $\text{atm}^{-1}$ , below the value ( $\sim 10^5 \text{ M atm}^{-1}$ ) needed for the majority of MDA to partition into cloud  
69 and fog droplets. Their model predicted that 8-9% of gas phase MDA would partition into a  
70 pH 6 fog droplet when  $[\text{MDA}] = 10^{-10} \text{ ppb}$ , but that by pH 2, partitioning would be negligible.  
71 This pH dependence is understood by recognizing that aqueous malondialdehyde prefers the  
72 enol form (Fig. 1a),  $\text{pK}_a = 4.7$ , which is more soluble than the dicarbonyl; at low pH the  
73 dialdehyde is favored, reducing its solubility substantially. Their model further predicts that  
74 MDA complexation of Cu(II) and Ni(II) at the droplet surface would enhance MDA  
75 partitioning (Okochi and Brimblecombe, 2002).

76 MDA has most commonly been measured in biological and other systems via  
77 derivatization with thiobarbituric acid (TBA) (Halliwell and Gutteridge 1981, Gutteridge and  
78 Halliwell 1988, Genaro-Mattos et al. 2009), the approach used here. The method reacts two  
79 TBA molecules with MDA, in the presence of acid and heat to form a  $\text{TBA}_2\text{-MDA}$  adduct that  
80 can be measured with absorption or fluorescence spectroscopy (Fig. 1, reaction 2).  
81 Interferences have been reported from MDA precursors such as carbohydrates that can form  
82 small amounts of  $(\text{TBA})_2\text{-MDA}$  upon heating, and from other carbonyls that form non-MDA  
83 adducts with TBA and absorb or fluoresce at similar wavelengths (Waravdekar and Saslaw  
84 1959, Morales and Munné-Bosch 2019). Such interferences are greatly reduced by using high  
85 performance liquid chromatography (HPLC) or mass spectrometry to detect  $\text{TBA}_2\text{-MDA}$   
86 (Moselhy et al. 2013, Domijan et al. 2015).

87            Here, for the first time, we apply the TBA method to estimate MDA concentrations in  
88 urban and biomass burning aerosols (BBA) particles smaller than 2.5 microns in diameter  
89 (PM<sub>2.5</sub>). We also characterize the fluorescence of the extracts with detailed excitation-emission  
90 (EEM) scans and investigate the potential of seven small oxygenated species common in the  
91 atmosphere for their potential to interfere with the MDA signal in the TBA assay.

92

## 93 **2. METHODS**

### 94 **2.1 Materials**

95            Malondialdehyde tetrabutyl ammonium salt ( $\geq 96\%$ ), 2-thiobarbituric acid ( $\geq 96\%$ ),  
96 acrolein (analytical standard), formaldehyde (36.5%-37.5% in water), sodium formate  
97 (99.9%), and oxalic acid (99.9%) and sodium malonate dibasic monohydrate (Bioextra) were  
98 purchased from Sigma-Aldrich. 0.1 N sulfuric acid was purchased from Titripur®. HPLC-  
99 grade acetonitrile was purchased from Omnisolve. HPLC-grade methanol was purchased from  
100 Fischer Scientific, and 15mL Falcon tubes (Corning Brand) were obtained from Thermo  
101 Scientific. Ultra-high purity Argon and Nitrogen were purchased from AirGas. Glyoxal (40%  
102 in water) and methylglyoxal (40% in water) were purchased from Tokyo Chemical Industry.

### 103 **2.2 Aerosol Sample Collection**

104            Four ambient PM<sub>2.5</sub> aerosol samples are tested here, one from Fresno (36.82 °N, 119.74  
105 °W) and three from Los Angeles, CA (34.07° N, 118.44° W). The Fresno sample contained  
106 mixed urban aerosol mixed with biomass burning aerosol from residential wood burning in the  
107 surrounding areas, and was collected on an a 406 cm<sup>2</sup> Teflon-coated glass fiber filter from Sept  
108 10 – 16, 2015 (Gonzalez et al. 2017). Urban PM<sub>2.5</sub> from Los Angeles, CA (Urban LA) was  
109 collected on the roof of the Math Sciences Building at UCLA. Urban LA samples were

110 collected on acid washed and pre-weighed PTFE filters (PALL, 47 mm 2  $\mu\text{m}$  pore size) using  
111 an URG cyclone at 92.5 L  $\text{Min}^{-1}$ , corresponding to a cut size of 2.5 microns. Three samples  
112 and three blanks were collected for approximately 24 hours each during March 27<sup>th</sup>-30<sup>th</sup> 2019.  
113 The mass of collected particles was determined immediately after collection using a  
114 microbalance (1  $\mu\text{g}$  precision, ME 5, Sartorius). To remove charge on the PTFE filters, a charge  
115 neutralizer was passed over the filter for 30 seconds before weighing. The Fresno BBA sample  
116 mass 467  $\mu\text{g in}^{-2}$ , corresponding to average PM concentrations of 3.0  $\mu\text{g m}^{-3}$ , of which about  
117 270  $\mu\text{g in}^{-2}$  was BBA. The content of BBA was characterized with optical absorption using an  
118 aethalometer (Paulson et al. 2019). The fraction of the sample comprised of BBA is at the  
119 higher end of observed BBA fraction compared to earlier measurements in Fresno (Paulson et  
120 al. 2019). The three urban LA samples had PM masses of 201  $\mu\text{g}$ , 551  $\mu\text{g}$ , and 835  $\mu\text{g}$ ,  
121 corresponding to average PM concentrations of 1.5  $\mu\text{g m}^{-3}$ , 4.1  $\mu\text{g m}^{-3}$ , and 6.3  $\mu\text{g m}^{-3}$   
122 respectively (Table 1). These values are on the low end for the West Los Angeles site, but such  
123 low values are common in the spring.

### 124 **2.3 Application of the 2-Thiobarbituric Acid Method to Measure MDA in Ambient $\text{PM}_{2.5}$**

125  $\text{PM}_{2.5}$  filter samples and blanks were placed in 15 mL Falcon tubes and extracted in 7.5 mL  
126 HPLC-grade methanol for 1 hour at room temperature in the dark. The extraction volume and  
127 time were chosen to allow all soluble organic constituents to dissolve. Extracting samples in  
128 the dark minimizes the possibility of photochemical reactions that may change the composition  
129 of the aerosol extract. Methanol was selected because it is a good solvent for small oxygenates  
130 and evaporates easily. The filters were then removed, and the methanol extracts were  
131 evaporated to dryness using a gentle stream of  $\text{N}_2$  at room temperature and reconstituted in 720  
132  $\mu\text{L}$  of milliQ water (adjusted to pH 3 with  $\text{H}_2\text{SO}_4$ ), followed by addition of 4 mM TBA (30  $\mu\text{L}$   
133 of 100 mM TBA), and incubation at 100°C for 1.25 hours. 2.4 Estimation of Malondialdehyde  
134 using 2-Thiobarbituric Acid

135 A wide variety of protocols have been reported for HPLC-fluorescence detection of  
136 TBA<sub>2</sub>-MDA in biological samples, but no protocols for the TBA assay applied to PM extracts  
137 were available. We performed quantification of TBA<sub>2</sub>-MDA using High-Performance Liquid  
138 Chromatography (HPLC) with a fluorescence detector (Shimadzu RF-10AXL). A reversed  
139 phase C-18 chromatography column (GL Sciences Inc., Intersil ODS-2, 5 μm, 4.6 x 250 mm)  
140 and guard column (Thermo Scientific, ODS Hypersil JAVELIN Filter, 5 μm, 4 x 10 mm)  
141 separated analytes, and peaks were analyzed with Chromperfect Software (Justice Laboratory  
142 Software). Because the TBA<sub>2</sub>-MDA adduct is most stable under acidic conditions (pH 2-3)  
143 (Guillén-Sans et al. 1997) and an eluent of 7:3 acetone:milli-Q water (18MΩ) acidified to  
144 pH 3 (with 0.1 N sulfuric acid) was suggested by Fukunaga et al. (1995), we performed the  
145 assay at pH 3. The eluent was continuously degassed with a gentle stream of argon and  
146 delivered at a rate of 1.0 mL min<sup>-1</sup>. The TBA<sub>2</sub>-MDA adduct eluted at 6 minutes, and  
147 fluorescence was measured at E<sub>x</sub>/E<sub>m</sub> = 530 nm/550nm.

148 The HPLC was calibrated daily with four MDA standards ranging from 0.25 to 2.5 μM.  
149 The method detection limit was about 0.1 μM. A typical TBA<sub>2</sub>-MDA calibration curve is  
150 shown in Figure 2a; calibration slopes were within ± 12% of one another. Calibration standards  
151 were prepared from pH 3 stock solutions of 100 mM TBA and 20 mM malondialdehyde  
152 tetrabutylammonium salt serially diluted to 20 μM MDA. TBA stock solution was prepared in  
153 a Teflon bottle with stirring and heating (90°C) for approximately 15 minutes until all TBA  
154 was dissolved. The TBA was used immediately after preparation because precipitants form  
155 approximately 20 minutes after removal from the hot plate. 30 μL TBA was added to 626 - 711  
156 μL pH3 MilliQ water, then 9.4 – 94 μL aliquots of the 20 μM MDA stock solution were added  
157 for a total volume of 750 μL. The resulting solutions were capped and incubated in a boiling  
158 water bath (100 °C for 1.25 hours, after which the calibration solutions turned a pink-purple

159 color; blanks did not change color. Solutions were cooled in a refrigerator at 4 °C for 15 minutes  
160 and analyzed with the HPLC immediately.

### 161 **2.3 Excitation-Emission Matrix Spectra and Interfering Compounds (3D Fluorescence)**

162 The Excitation-Emission Matrix (EEM) scan mode (Lumina Fluorometer, Thermo  
163 Scientific) was used to determine fluorescence features of MDA calibrations, BBA extracts,  
164 PM samples and potential interfering compounds. Scans were performed every 5 nm in both  
165 excitation and emission space, using 10 nm excitation and emission slit widths and 20 ms  
166 integration time for each step. The instrument scanned at 60 nm per second. Figure 3 shows an  
167 EEM for a 1  $\mu$ M MDA standard after reaction with 4 mM TBA. Fluorescence contours indicate  
168 a fluorophore with peak fluorescence centered at  $E_x/E_m = 530 \text{ nm}/550\text{nm}$ , corresponding to the  
169 TBA<sub>2</sub>-MDA adduct (Del Rio et al. 2005, Moselhy et al. 2013, Domijan et al. 2015).

170 To characterize potential interfering compounds, we made 10 mM solutions of  
171 formaldehyde, formate, oxalic acid, malonate, glyoxal, methylglyoxal, and acrolein and  
172 incubated them in the presence of 4 mM of TBA adjusted to pH 3 (with H<sub>2</sub>SO<sub>4</sub>) heated at 100°C  
173 for 1.25 hrs.

174

## 175 **3. RESULTS AND DISCUSSION**

### 176 **3.1 Malondialdehyde in Fresno BBA and Los Angeles PM<sub>2.5</sub>**

#### 177 **3.1.1 Concentrations**

178 All HPLC analyses of the derivatized PM extracts exhibited a signal that matched that  
179 of the MDA standards, with a retention time of 6 minutes and fluorescence at  $E_x/E_m = 530/550$   
180 nm, indicating the presence of TBA<sub>2</sub>-MDA. We used varying amounts of the Fresno PM



181 sample to test dependence of the signal on aerosol mass and found a linear relationship (Fig.  
182 2b). The estimated concentration of MDA in the Fresno sample was  $0.31 \pm 0.02 \text{ ng m}^{-3}$  or  $(10.2$   
183  $\pm 0.6) \times 10^{-3} \text{ ng MDA } (\mu\text{g PM})^{-1}$  (Figure 4). Urban LA samples contained 51 to 97ng MDA  
184 corresponding to approximately 0.41, 0.75, and 0.55  $\text{ng m}^{-3}$  or 0.25, 0.18, and 0.087  $\text{ng } \mu\text{g}^{-1}$   
185 respectively (Tab. 1 and Fig. 4).

186 While we were unable to find reports of MDA concentrations in urban aerosols, we can  
187 compare concentration measurements to the concentrations of similar  $\text{C}_3$  oxygenated organic  
188 compounds in ambient urban  $\text{PM}_{2.5}$  (Destailats et al. 2002, Ho et al. 2010, Kawamura et al.  
189 2013, He et al. 2014, Ho et al. 2015, Shen et al. 2018). Reported concentrations for  
190 methylglyoxal, the 1, 2-carbonyl isomer of MDA (Fig. 1c), range from 0.8 – 242  $\text{ng m}^{-3}$  in  
191 urban  $\text{PM}_{2.5}$  (Destailats et al. 2002, Ho et al. 2010, Kawamura et al. 2013, He et al. 2014, Ho  
192 et al. 2015, Shen et al. 2018). Malonic acid, a structurally similar molecule containing two  
193 carboxylic acids instead of two aldehyde groups (Fig. 1c; we note that there is no known  
194 pathway for oxidation of MDA to form malonic acid in the atmosphere), has been reported at  
195 concentrations in the range 17.6 - 233  $\text{ng m}^{-3}$  in urban  $\text{PM}_{2.5}$  (Ho et al. 2010, He et al. 2014,  
196 Ho et al. 2015). Thus, our reported range of 0.31 – 0.75  $\text{ng m}^{-3}$  MDA are similar to the low  
197 end of methylglyoxal and up to three orders of magnitude lower than the upper limits of the  
198 concentrations of both methylglyoxal and malonic acid.

### 199 3.1.2 EEM Scans of Fresno BBA and Los Angeles $\text{PM}_{2.5}$

200 Figure 5a shows an EEM of the extract of 467  $\mu\text{g}$  of Fresno  $\text{PM}_{2.5}$ , without addition of  
201 TBA. While urban samples typically do not exhibit fluorescence, the biomass burning HUmic-  
202 Like Substances (HULIS) in the Fresno sample are strongly fluorescent. The sample's two  
203 peaks centered at  $E_x/E_m = 350/460 \text{ nm}$  and  $E_x/E_m = 330/410 \text{ nm}$  are characteristic of HULIS,  
204 and are similar to Fulvic Acids (Graber and Rudich 2006, Kuang 2017). Figure 5b shows an

205 EEM scan for the same Fresno sample reacted with 4 mM TBA. After processing, the sample  
206 retains some of the fluorescence features of HULIS and gains a fluorescent feature matching  
207 the TBA<sub>2</sub>-MDA fluorophore centered at  $E_x/E_m = 530/550$  nm. Interestingly, there is another  
208 fluorophore centered at  $E_x/E_m = 455/470$  nm with a similar trapezoidal shape as the TBA<sub>2</sub>-  
209 MDA fluorophore. This fluorophore could arise from a TBA-aldehyde adduct of a different  
210 dicarbonyl species. Possible identities for this species are discussed below.

211         Figures 6a-c show EEM scans of the three concentrated Urban LA PM<sub>2.5</sub> extracts after  
212 reaction with 4 mM TBA. Concentrated extracts of Urban LA PM<sub>2.5</sub> without addition of TBA  
213 had no observable fluorescence. EEMs for all three samples show the characteristic  
214 fluorescence of the TBA<sub>2</sub>-MDA adduct centered at  $E_x/E_m = 530/550$  nm. Additional  
215 trapezoidal-shaped peaks are also observed in these samples, including the same  $E_x/E_m =$   
216  $455/470$  nm peak observed in the Fresno sample, and a second satellite peak at  $E_x/E_m = 640/665$   
217 nm.

218         While TBA may react with many aldehydes, the formation of a fluorophore requires  
219 addition of two TBA molecules, forming a conjugated system connecting the two aromatic  
220 rings, a system that is only possible for molecules with odd numbers of carbon atoms in the  
221 backbone and two aldehyde groups. However, despite running the TBA assay on multiple C<sub>1</sub>  
222 – C<sub>3</sub> oxygenated compounds (Fig. 1c) we were not able to produce any fluorescence features  
223 other than the one matching MDA, and that was only observed in trace quantities for acrolein  
224 (below). Generally, any substitution in the fluorophore will red-shift the peak, suggesting that  
225 the peak at 640/655 nm could be from methyl malondialdehyde (methylpropanedial) or another  
226 malondialdehyde with a substitution at the center carbon. The explanation for the peak at  
227 455/470 nm is less clear, although its wavelengths might suggest one carbon bridging the two  
228 aromatic rings rather than three.

## 229 3.2 Potential Interferences with the TBA Assay

### 230 3.2.1 Other Small Oxygenates

231 We tested the common small oxygenates expected in ambient samples for their ability  
232 to react with TBA and produce a product with the same or similar fluorescence characteristics  
233 as the MDA-TBA<sub>2</sub> adduct. Formaldehyde, formic acid, oxalic acid, malonate, glyoxal and  
234 methylglyoxal (Fig. 1c) produced no measurable fluorescence anywhere in the E<sub>x</sub>/E<sub>m</sub> spectrum.  
235 Of all compounds tested, only acrolein produced any measurable fluorescence. The signal for  
236 acrolein appears at the same retention time in the HPLC and has the same fluorescence features  
237 as the TBA<sub>2</sub>-MDA adduct. Triplicate samples of 1 mM and 10 mM acrolein were reacted with  
238 4 mM TBA under oxygenated conditions produced  $0.45 \pm 0.07 \mu\text{M}$  and  $0.87 \pm 0.2 \mu\text{M}$  MDA  
239 respectively, corresponding to 0.004% -0.008% conversion of acrolein to MDA. As it is  
240 unlikely that acrolein would make up more than a few % of aerosol mass, acrolein is unlikely  
241 to contribute measurably to the TBA<sub>2</sub>-MDA signals for the aerosol extracts.

242 The MDA associated with acrolein may have been present in the bottle from the  
243 manufacturer, or it may have been produced via acid hydration of the acrolein followed by  
244 oxidation, as proposed in Figure 7. Under this mechanism, protonation of the alkene group  
245 produces a primary and secondary carbocation, followed hydration that produces 2-  
246 hydroxypropanal and 3-hydroxypropanal. Two possible oxidation products of these hydration  
247 products are glyoxal and MDA. The hydration of acrolein to 3-hydroxypropanal has been  
248 identified under acidic conditions (Pressman and Lucas 1942, Melicherčík and Treindl 1981,  
249 Campadelli et al. 1983), but we could find no studies identifying MDA as a product of acrolein  
250 hydration and oxidation. Furthermore, primary carbocations are known to be less stable than  
251 secondary carbocations. Thus, formation of MDA from acrolein should be a minor pathway,  
252 consistent with the very low observed yield.

### 253 3.2.2 Reactive Oxygen Species and Potential Formation of MDA in the Assay

254           There is some potential for formation of MDA in the assay itself. This would most  
255 likely happen via an oxidation reaction, mediated by hydroxyl radicals or other reactive oxygen  
256 species. Any hydroxyl radicals or other reactive oxygen species that might form during the  
257 heating phase of the assay should be scavenged by the large excess (4 mM) of TBA in the  
258 solution. Nonetheless, for some calibration samples, a gentle stream of argon was bubbled  
259 through the solution for approximately 1 minute prior to TBA addition and incubation to  
260 remove oxygen and reduce ROS generation during the assay. No differences were observed  
261 (data not shown), indicating that oxygen does not impact the condensation reaction between  
262 TBA and MDA, and ROS did not affect the calibration.

### 263 3.3 Potential Sources of Atmospheric MDA

264           MDA in particles could arise via reactions on the particles themselves, or partitioning  
265 from the gas phase, either directly into the particles or into cloud or fog droplets followed by  
266 incorporation into the particles once the droplet re-evaporates. Liu et al. (1999) reported  
267 formation of malondialdehyde from gas phase photo-oxidation of butadiene and unsaturated  
268 dicarbonyls. The Henry's law coefficient of methylglyoxal (and several other aldehydes)  
269 estimated from recent field measurements indicate that the Henry's Law partitioning  
270 coefficient for methylglyoxal could be  $\sim 10^8 \text{ M atm}^{-1}$ , much higher than values reported earlier  
271 ( $\sim 10^4 \text{ M atm}^{-1}$ ) (Betterton and Hoffmann 1988, Lee and Zhou 1993, Shen et al. 2018). Since  
272 MDA and methylglyoxal have similar theoretical Henry's Law constants ( $\sim 10^4 - 10^5 \text{ M atm}^{-1}$ )  
273 (Okochi and Brimblecombe 2002, Shen et al. 2018) and similar molecular structures, it is  
274 possible that they share similar gas-particle partitioning behavior. MDA has a higher boiling  
275 point (108 °C) than methylglyoxal (72 °C), and thus may partition into the aqueous phase even  
276 more readily than methylglyoxal. Further potentially enhancing partitioning is the formation of

277 the enol form (above the  $pK_a$  of 4.7) although this is expected to be more likely to play a role  
278 in clouds and fog, as aerosols are believed to often be too acidic (pH 0 – 2) for this to be relevant  
279 (Weber et al. 2016). MDA complexation to Cu(II) and Ni(II) at the droplet surface may also  
280 enhance MDA uptake (Okochi and Brimblecombe 2002).

281 It is also possible that reactions photochemical (Beeby et al. 1987) or dark oxidation  
282 reactions within aerosol waters result in MDA production. MDA is expected as an oxidation  
283 product from 1,4 dienes, and 1, 3 unsaturated aldehydes; and it has been observed as an  
284 oxidation product of butadiene oxidation (Liu et al. 1999, Liu et al. 1999). Further,  
285 polyunsaturated fatty acids are MDA precursors in biological systems, and it is well  
286 documented that aqueous oxidation of 2-deoxyribose sugar produces MDA (Halliwell and  
287 Gutteridge 1981, Gutteridge and Halliwell 1988). Atmospheric aerosols contain some  
288 biological material, including whole or fragmented bacteria and viruses, and fragments of plant  
289 material, material that is composed of a variety of polyunsaturated fatty acids and  
290 polysaccharides such as cellulose, hemicellulose, lignin, and free sugars including deoxyribose.

### 291 **3.4 MDA Toxicity**

292 MDA has been classified as a potential occupational carcinogen, although no reference  
293 exposure limits (RELs) have been established (NIOSH 1990). Many small aldehydes exhibit  
294 toxicity, although their reference exposure limits vary widely; the reference limits for chronic  
295 exposure range from  $0.35 \mu\text{g m}^{-3}$  for acrolein, 9 for formaldehyde and  $140 \mu\text{g m}^{-3}$  for  
296 acetaldehyde (OEHHA 2021). While the REL for acrolein is in the same range as our  
297 measurements of MDA in the particle phase, it has yet to be established that MDA is as toxic  
298 as acrolein. The MDA concentrations in the particle phase are significantly lower than the  
299 RELs for formaldehyde and acetaldehyde. Future studies should aim to measure both gas and  
300 particle phase MDA concentrations for toxicology assessment.

### 301 **3.5 Conclusions**

302           The thiobarbituric acid assay has been successfully applied to measure MDA in ambient  
303 aerosol particles. Other compounds found in aerosols do not appear to present significant  
304 interferences for the assay. Levels of MDA in urban samples, including one containing a  
305 significant contribution from biomass burning, were moderate at  $\sim 0.5 \text{ ng m}^{-3}$ . This  
306 concentration is at the low end of observed concentrations of similar small carbonyl compounds  
307 in ambient aerosols, but it may contribute to toxicity of ambient air in combination with gas-  
308 phase MDA and other toxic species.

309

### 310 **ACKNOWLEDGEMENTS**

311 The authors gratefully acknowledge Prof. Alam Hasson of the California State University,  
312 Fresno for the BBA sample used in this work. We thank J. Adlin Scott for measurement of  
313 BBA in the Fresno sample. We thank J. Puna Bauman for assistance in some of the preliminary  
314 experiments leading to this work.

### 315 **DISCLAIMER**

316 The authors have no disclaimers to disclose.

### 317 **REFERENCES**

- 318 Agarwal, A. and A. Majzoub (2017). "Laboratory tests for oxidative stress." Indian journal of urology:  
319 IJU: journal of the Urological Society of India **33**(3): 199.  
320 Basu, A. K. and L. J. Marnett (1983). "Unequivocal demonstration that malondialdehyde is a  
321 mutagen." Carcinogenesis **4**(3): 331-333.  
322 Beeby, A., D. b. H. Mohammed and J. R. Sodeau (1987). "Photochemistry and photophysics of  
323 glycolaldehyde in solution." Journal of the American Chemical Society **109**(3): 857-861.

- 324 Betterton, E. A. and M. R. Hoffmann (1988). "Henry's law constants of some environmentally  
325 important aldehydes." Environmental science & technology **22**(12): 1415-1418.
- 326 Buege, J. A. and S. D. Aust (1978). [30] Microsomal lipid peroxidation. Methods in enzymology,  
327 Elsevier. **52**: 302-310.
- 328 Campadelli, F., C. Tosi, E. Santoro and L. Roberti (1983). "Spectroscopic investigation on the acrolein  
329 hydration." Spectroscopy letters **16**(8): 601-611.
- 330 Del Rio, D., A. J. Stewart and N. Pellegrini (2005). "A review of recent studies on malondialdehyde as  
331 toxic molecule and biological marker of oxidative stress." Nutrition, metabolism and cardiovascular  
332 diseases **15**(4): 316-328.
- 333 Destailats, H., R. S. Spaulding and M. J. Charles (2002). "Ambient air measurement of acrolein and  
334 other carbonyls at the Oakland-San Francisco Bay Bridge toll plaza." Environmental science &  
335 technology **36**(10): 2227-2235.
- 336 Domijan, A. M., J. Ralić, S. Radić Brkanac, L. Rumora and T. Žanić-Grubišić (2015). "Quantification of  
337 malondialdehyde by HPLC-FL—application to various biological samples." Biomedical  
338 Chromatography **29**(1): 41-46.
- 339 Fukunaga, K., K. Takama and T. Suzuki (1995). "High-performance liquid chromatographic  
340 determination of plasma malondialdehyde level without a solvent extraction procedure." Analytical  
341 biochemistry **230**(1): 20-23.
- 342 Genaro-Mattos, T. C., L. T. Dalvi, R. G. Oliveira, J. S. Ginani and M. Hermes-Lima (2009).  
343 "Reevaluation of the 2-deoxyribose assay for determination of free radical formation." Biochimica et  
344 Biophysica Acta (BBA)-General Subjects **1790**(12): 1636-1642.
- 345 Gonzalez, D. H., C. K. Cala, Q. Peng and S. E. Paulson (2017). "HULIS Enhancement of Hydroxyl  
346 Radical formation from Fe (II): Kinetics of Fulvic Acid-Fe (II) Complexes in the Presence of Lung Anti-  
347 Oxidants." Environmental Science & Technology.
- 348 Graber, E. and Y. Rudich (2006). "Atmospheric HULIS: How humic-like are they? A comprehensive  
349 and critical review." Atmospheric Chemistry and Physics **6**(3): 729-753.
- 350 Guillén-Sans, R., I. Vicario and M. Guzmán-Chozas (1997). "Further studies and observations on 2-  
351 thiobarbituric acid assay (fat autoxidation) and 2-thiobarbituric acid-aldehyde reactions."  
352 Food/Nahrung **41**(3): 162-166.
- 353 Gutteridge, J. and B. Halliwell (1988). "The deoxyribose assay: an assay both for 'free' hydroxyl radical  
354 and for site-specific hydroxyl radical production." Biochemical Journal **253**(3): 932.
- 355 Halliwell, B. and J. Gutteridge (1981). "Formation of a thiobarbituric-acid-reactive substance from  
356 deoxyribose in the presence of iron salts." FEBS letters **128**(2): 347-352.
- 357 He, N., K. Kawamura, K. Okuzawa, P. Pochanart, Y. Liu, Y. Kanaya and Z. Wang (2014). "Diurnal and  
358 temporal variations of water-soluble dicarboxylic acids and related compounds in aerosols from the  
359 northern vicinity of Beijing: Implication for photochemical aging during atmospheric transport."  
360 Science of the Total Environment **499**: 154-165.
- 361 Ho, K., R.-J. Huang, K. Kawamura, E. Tachibana, S. Lee, S. Ho, T. Zhu and L. Tian (2015). "Dicarboxylic  
362 acids, ketocarboxylic acids,  $\alpha$ -dicarbonyls, fatty acids and benzoic acid in PM 2.5 aerosol collected  
363 during CAREBeijing-2007: an effect of traffic restriction on air quality." Atmospheric Chemistry and  
364 Physics **15**(6): 3111-3123.
- 365 Ho, K., S. Lee, S. S. H. Ho, K. Kawamura, E. Tachibana, Y. Cheng and T. Zhu (2010). "Dicarboxylic acids,  
366 ketocarboxylic acids,  $\alpha$ -dicarbonyls, fatty acids, and benzoic acid in urban aerosols collected during  
367 the 2006 Campaign of Air Quality Research in Beijing (CAREBeijing-2006)." Journal of geophysical  
368 research: atmospheres **115**(D19).
- 369 Kawamura, K., K. Okuzawa, S. Aggarwal, H. Irie, Y. Kanaya and Z. Wang (2013). "Determination of  
370 gaseous and particulate carbonyls (glycolaldehyde, hydroxyacetone, glyoxal, methylglyoxal, nonanal  
371 and decanal) in the atmosphere at Mt. Tai." Atmospheric Chemistry and Physics **13**(10): 5369-5380.
- 372 Kuang, X. M. (2017). Formation of Reactive Oxygen Species by Ambient Particulate Matter: Probing  
373 causative agents and the underlying mechanism, UCLA.

- 374 Lee, Y. N. and X. Zhou (1993). "Method for the determination of some soluble atmospheric carbonyl  
375 compounds." Environmental science & technology **27**(4): 749-756.
- 376 Liu, X., H. E. Jeffries and K. G. Sexton (1999). "Atmospheric photochemical degradation of 1, 4-  
377 unsaturated dicarbonyls." Environmental science & technology **33**(23): 4212-4220.
- 378 Liu, X., H. E. Jeffries and K. G. Sexton (1999). "Hydroxyl radical and ozone initiated photochemical  
379 reactions of 1, 3-butadiene." Atmospheric Environment **33**(18): 3005-3022.
- 380 Melicherčík, M. and L. Treindl (1981). "Kinetics and mechanism of the oxidation of acrolein,  
381 crotonaldehyde, and methacrolein with cerium (IV) sulfate." Chemical Papers **35**(2): 153-163.
- 382 Millar, J. D. (1991). "Carcinogenicity of acetaldehyde and malonaldehyde, and mutagenicity of  
383 related low-molecular-weight aldehydes."
- 384 Morales, M. and S. Munné-Bosch (2019). "Malondialdehyde: facts and artifacts." Plant physiology  
385 **180**(3): 1246-1250.
- 386 Moselhy, H. F., R. G. Reid, S. Yousef and S. P. Boyle (2013). "A specific, accurate, and sensitive  
387 measure of total plasma malondialdehyde by HPLC." Journal of lipid research **54**(3): 852-858.
- 388 Niedernhofer, L. J., J. S. Daniels, C. A. Rouzer, R. E. Greene and L. J. Marnett (2003).  
389 "Malondialdehyde, a product of lipid peroxidation, is mutagenic in human cells." Journal of Biological  
390 Chemistry **278**(33): 31426-31433.
- 391 NIOSH (1990). Title 29 Code of Federal Regulations Part 1990 DHHS (NIOSH) Publication Number 91-  
392 112.
- 393 OEHHA (2021). OEHHA Acute, 8-hour and Chronic Reference Exposure Level (REL) Summary.  
394 Sacramento, CA, USA.
- 395 Okochi, H. and P. Brimblecombe (2002). "Potential trace metal–organic complexation in the  
396 atmosphere." The Scientific World Journal **2**: 767-786.
- 397 Papac-Milicevic, N., C.-L. Busch and C. J. Binder (2016). "Malondialdehyde epitopes as targets of  
398 immunity and the implications for atherosclerosis." Advances in immunology **131**: 1-59.
- 399 Paulson, S. E., P. J. Gallimore, X. M. Kuang, J. R. Chen, M. Kalberer and D. H. Gonzalez (2019). "A  
400 light-driven burst of hydroxyl radicals dominates oxidation chemistry in newly activated cloud  
401 droplets." Science Advances **5**(5): eaav7689. DOI: 10.1126/sciadv.aav7689.
- 402 Pressman, D. and H. Lucas (1942). "Hydration of Unsaturated Compounds. XI. Acrolein and Acrylic  
403 Acid1." Journal of the American Chemical Society **64**(8): 1953-1957.
- 404 Shen, H., Z. Chen, H. Li, X. Qian, X. Qin and W. Shi (2018). "Gas-Particle Partitioning of Carbonyl  
405 Compounds in the Ambient Atmosphere." Environmental Science & Technology **52**(19): 10997-  
406 11006. DOI: 10.1021/acs.est.8b01882.
- 407 Waravdekar, V. and L. Saslaw (1959). "A sensitive colorimetric method for the estimation of 2-deoxy  
408 sugars with the use of the malonaldehydethiobarbituric acid reaction." Journal of Biological  
409 Chemistry **234**(8): 1945-1950.
- 410 Weber, R. J., H. Guo, A. G. Russell and A. Nenes (2016). "High aerosol acidity despite declining  
411 atmospheric sulfate concentrations over the past 15 years." Nature Geoscience **9**(4): 282-285.
- 412 Zeb, A. and F. Ullah (2016). "A simple spectrophotometric method for the determination of  
413 thiobarbituric acid reactive substances in fried fast foods." Journal of analytical methods in  
414 chemistry **2016**.
- 415 Zhou, S., L. Gonzalez, A. Leithead, Z. Finewax, R. Thalman, A. Vlasenko, S. Vagle, L. Miller, S.-M. Li, S.  
416 Bureekul, H. Furutani, M. Uematsu, R. Volkamer and J. Abbatt (2014). "Formation of gas-phase  
417 carbonyls from heterogeneous oxidation of polyunsaturated fatty acids at the air–water interface  
418 and of the sea surface microlayer." Atmospheric Chemistry and Physics **14**(3): 1371-1384.

419

420

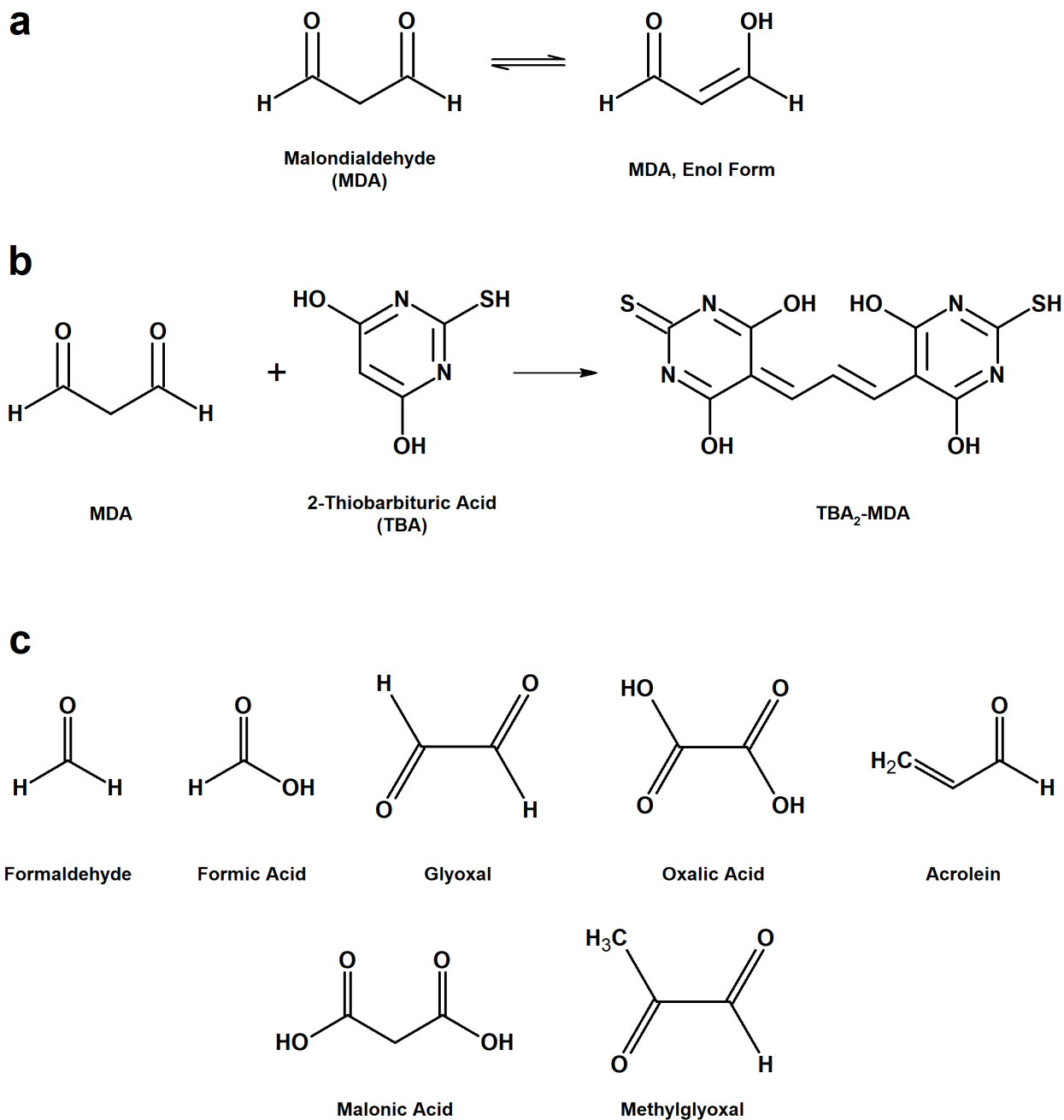


421  
422  
423  
424  
425  
426  
427  
428  
429  
430  
431

432 **TABLE 1. AMBIENT SAMPLE RESULTS**

<b>Sample</b>	<b>Aerosol Mass on filter (<math>\mu\text{g}</math>)<sup>a</sup></b>	<b>Aerosol Mass Conc. (<math>\mu\text{g}/\text{m}^3</math>)</b>	<b>MDA on filter (ng)</b>	<b>MDA Conc. (<math>\text{ng}/\text{m}^3</math>)</b>	<b>MDA per aerosol mass (<math>\text{ng}/\mu\text{g}</math>)</b>	<b>Fresno BBA content</b>
<b>Fresno</b> (Sept 10-16, 2015)	467	3	51	$0.33 \pm .02$	$0.11 \pm .01$	266
<b>Los Angeles 1</b> (Mar 27, 2019)	201	1.5	51	$0.41 \pm .02$	$0.25 \pm .01$	–
<b>Los Angeles 2</b> (Mar 28, 2019)	551	4.1	97	$0.75 \pm .01$	$0.18 \pm .01$	–
<b>Los Angeles 3</b> (Mar 29, 2019)	835	6.3	72	$0.55 \pm .06$	$0.09 \pm .01$	–

433 <sup>a</sup>Mass on whole 47 mm filter for LA samples; mass on 1" square punch from Fresno filter.  
434  
435



436

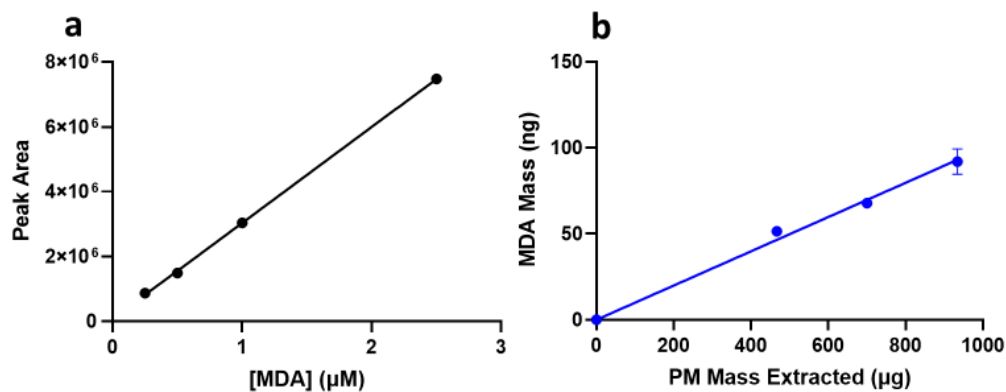
437 **Figure 1. (a)** Malondialdehyde aqueous equilibrium reaction. **(b)** Condensation Reaction of438 MDA and TBA to form TBA<sub>2</sub>-MDA. **(c)** C<sub>1</sub> – C<sub>3</sub> compounds tested for interference in the

439 TBA assay.

440

441

442



443

444 **Figure 2.** (a) Calibration curve for TBA<sub>2</sub>-MDA adduct measured with HPLC-Fluorescence.  
445 Peaks eluted at a retention time of 6 minutes. (b) Mass of MDA measured from TBA assay  
446 for different quantities of Fresno urban/biomass burning aerosol. Error bars indicate  $\pm 1\sigma$  of  
447 three values measured on the HPLC from the same sample extract.

448

449

450

451

452

453

454

455

456

457

458

459

460

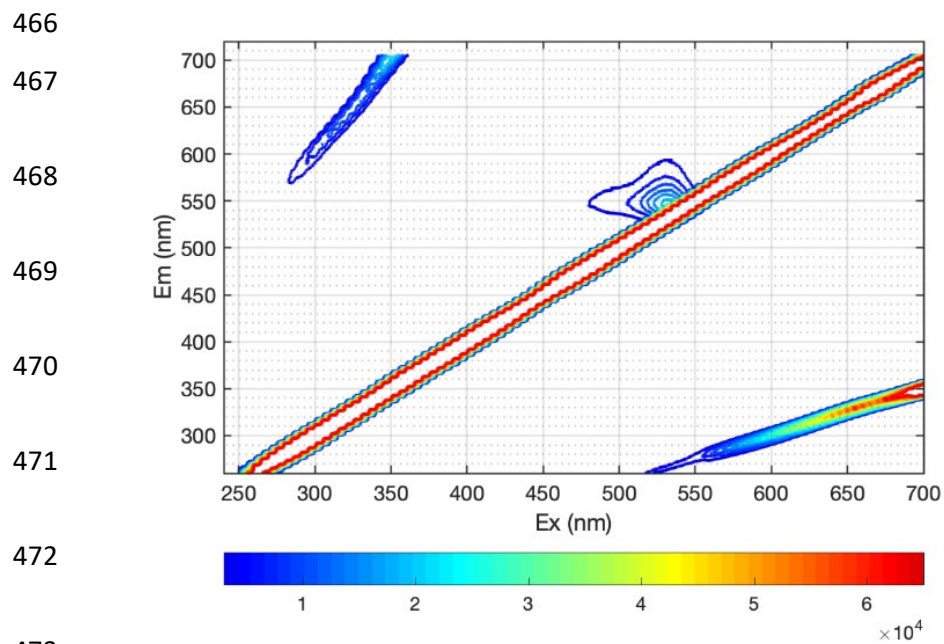
461

462

463

464

465



474 **Figure 3.** Excitation-emission matrix scan of 1  $\mu$ M MDA assayed with 4 mM TBA in pH 3.

475

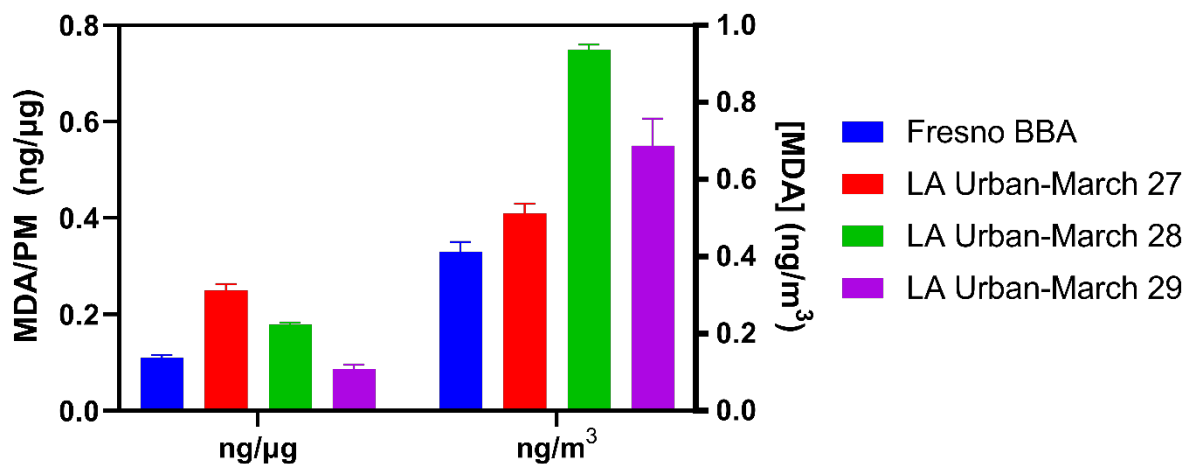
476

477

478

479

480



481

482 **Figure 4.** MDA measured with the TBA assay for the Fresno biomass burning aerosol (BBA,  
 483 blue bar) and urban Los Angeles PM<sub>2.5</sub> (Urban LA; red, green, and purple bars) extracts.

484 Error bars indicate  $\pm 1\sigma$  of three values measured on the HPLC from the same sample extract.

485

486

487

488

489

490

491

492

493

494

495

496

497

498

499

500

501

502

503

504

505

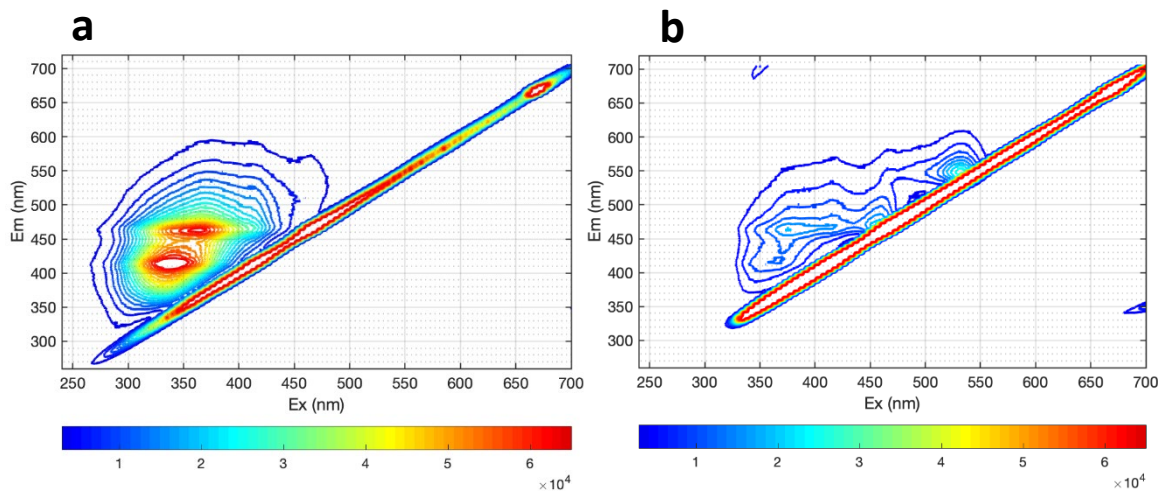
506

507

508

509

510



511 **Figure 5.** Excitation-emission matrix of (a) 467  $\mu\text{g}$  Fresno BBA extracted in methanol and  
512 reconstituted in aqueous pH 3 solution and (b) the same extract after reaction with 4 mM  
513 TBA.

514

515

516

517

518

519

520

521

522

523

524

525

526

527

528

529

530

531

532

533

534

535

536

537

538

539

540

541

542

543

544

545

546

547

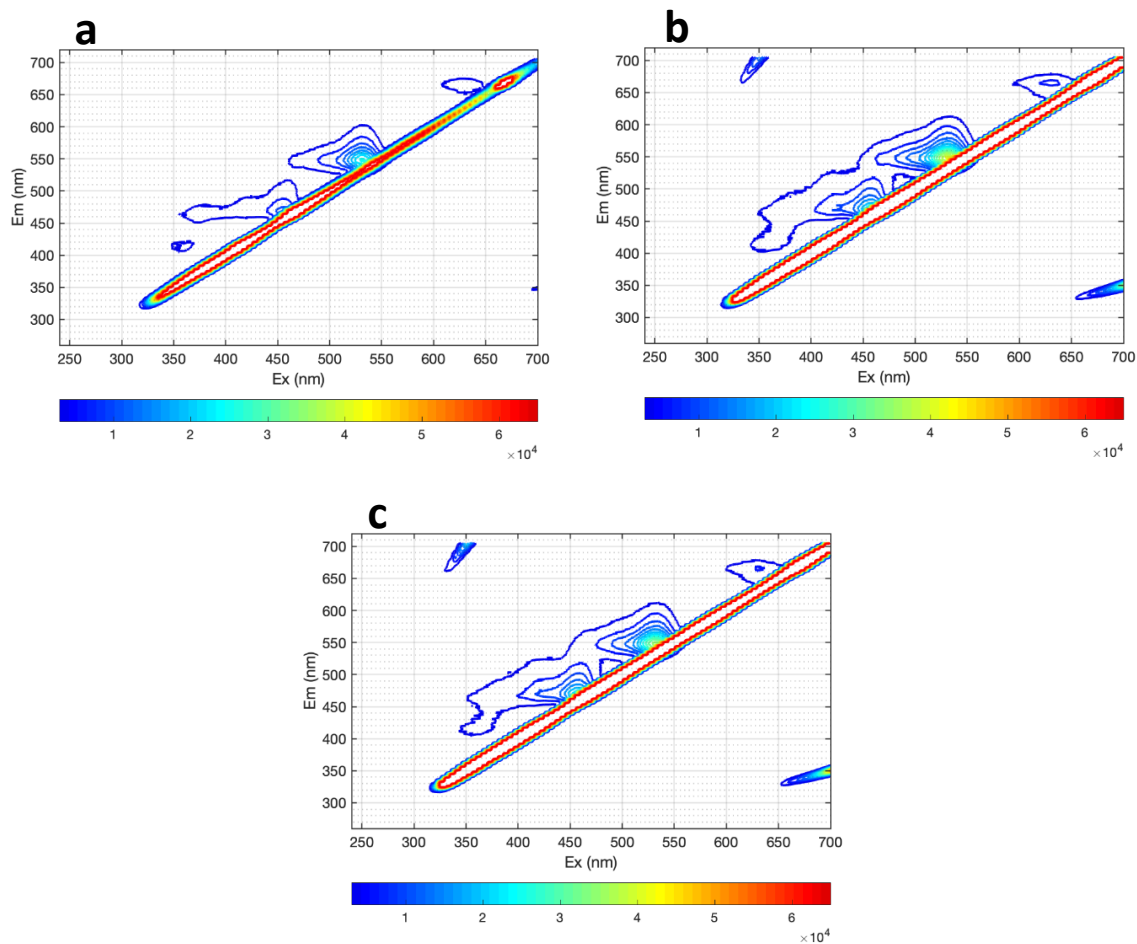
548

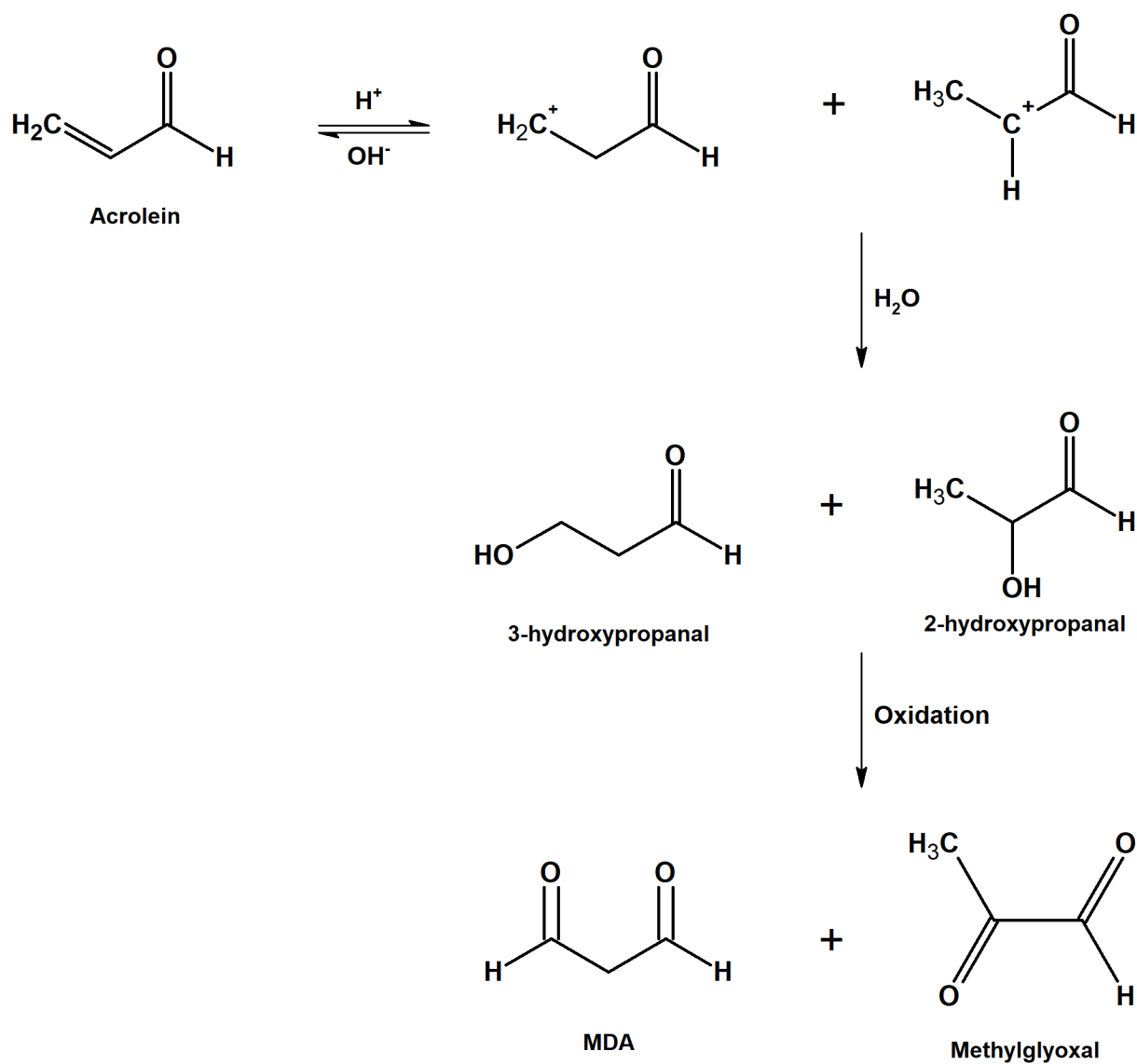
549

550

551 **Figure 6.** Excitation-emission matrix spectra for three urban Los Angeles PM<sub>2.5</sub> (samples  
 552 collected on different days) assayed with 4 mM TBA in aqueous pH 3 solution. The samples  
 553 had masses of (a) 201  $\mu\text{g}$  (c) 551  $\mu\text{g}$  (c) 835  $\mu\text{g}$  (Tab. 1). The diagonal features in the center  
 554 and at  $E_x/E_m \sim 680/320$  nm and  $320/650$  nm respectively are scattering artifacts inherent to  
 555 the spectrometer.

556





557

558 **Figure 7.** Proposed mechanism for conversion of acrolein to MDA under acidic, oxygenated  
 559 conditions.

560